© 2020. Published by The Company of Biologists Ltd | Development (2020) 147, dev184457. doi:10.1242/dev.184457

RESEARCH ARTICLE

Interplay of MPP5a with Rab11 synergistically builds epithelial apical polarity and zonula adherens

Yumei Hao[1,2,*], Yao Zhou[1,2,*], Yinhui Yu[1,*], Mingjie Zheng[1,2], Kechao Weng[1,2], Ziqi Kou[1,2], Jiancheng Liang[1,2], Qian Zhang[3], Xiajing Tang[1], Pinglong Xu[3], Brian A. Link[4], Ke Yao[1,5,‡] and Jian Zou[1,2,5,‡]

ABSTRACT

Adherens junction remodeling regulated by apical polarity proteins constitutes a major driving force for tissue morphogenesis, although the precise mechanism remains inconclusive. Here, we report that, in zebrafish, the Crumbs complex component MPP5a interacts with small GTPase Rab11 in Golgi to transport cadherin and Crumbs components synergistically to the apical domain, thus establishing apical epithelial polarity and adherens junctions. In contrast, Par complex recruited by MPP5a is incapable of interacting with Rab11 but might assemble cytoskeleton to facilitate cadherin exocytosis. In accordance, dysfunction of MPP5a induces an invasive migration of epithelial cells. This adherens junction remodeling pattern is frequently observed in zebrafish lens epithelial cells and neuroepithelial cells. The data identify an unrecognized MPP5a-Rab11 complex and describe its essential role in guiding apical polarization and zonula adherens formation in epithelial cells.

KEY WORDS: MPP5a, Rab11, Apical polarity, Adherens junctions remodeling, Zonula adherens

INTRODUCTION

Adherens junction (AJ) remodeling and cytoskeleton rearrangement are the major driving forces of cell migration and play essential roles, such as convergent extension and collective cell migration, in both organogenesis and diseases. Adapting to cell state, AJs can be assembled into three diverse modes – punctum adherens, zonula adherens and tricellular adherens – depending on the shape, position and mode of actin filament association with AJs (Yonemura, 2011), which endows the cells with the dual properties of rigidity and plasticity (Harris and Tepass, 2010; Balda and Matter, 2016). For instance, zonula adherens at the apical domain is the hallmark of epithelial cells and necessary to stabilize epithelial tissue.

Remodeling of AJs involves the activity of both the Rab family of small GTPases and cellular polarity proteins (Harris and Tepass, 2010; Bruser and Bogdan, 2017; Apodaca et al., 2012). Rab family proteins, which are known to control membrane identity and vesicle trafficking between organelles (Stenmark, 2009; Scott et al., 2014), participate in the recycling of AJs. Among these Rab proteins, Rab5 is crucial for the formation of the early endosome (Chavrier et al., 1990; Gorvel et al., 1991; Barbieri et al., 1996). The proteins internalized into early endosomes are sorted either for degradation in the endolysosomal pathway or for recycling. Rab11 functions as a key regulator in the recycling endosomes and in transport from the trans-Golgi network to the plasma membrane, which is crucial for establishing the apical zonula adherens in epithelial cells (Ullrich et al., 1996; Chen et al., 1998; Woichansky et al., 2016). However, how Rab11 guides the vesicles specifically to the apical domains of cells is still not well understood, although a series of Rab11-interacting proteins has previously been identified (Apodaca et al., 2012).

Rab11, a Rab family small GTPase and key trafficking regulator of AJ components, is associated with the cellular polarity complex (Harris and Tepass, 2008; Roeth et al., 2009; Bryant et al., 2010; Clark et al., 2011; Sobajima et al., 2014; Hosono et al., 2015). Rab11 is usually enriched at the apical domains in epithelial cells. The apical localization of Rab11 appears to need polarity proteins. For instance, atypical protein kinase C (aPKC), the key kinase in the Par6-Par3-aPKC-CDC42 (Par) complex, modulates the orientation of actomyosin cables to promote the Rab11-mediated exocytosis in *Drosophila* (Harris and Tepass, 2008; Hosono et al., 2015), and non-apical polarity protein Par5 functions as a regulatory hub for Rab11-positive recycling endosomes in *C. elegans* (Winter et al., 2012). Nevertheless, the regulatory protein(s) that drive Rab11-mediated apical vesicle trafficking in vertebrates have still not been identified.

The complexes of Crumbs (Crb)-MPP5a-PATJ and Par6-Par3-aPKC-CDC42 are the key determinants of epithelial apical polarity that function conservatively in multiple organs in species from *Drosophila* to mammals (Bulgakova and Knust, 2009; Tepass, 2012; Chen and Zhang, 2013). Both the Crb complex and the Par complex are required for AJ modeling in epithelial cells. Ablation of these complexes leads to similar defects in the formation of apical zonula adherens (Tepass, 1996; Klebes and Knust, 2000; Joberty et al., 2000; Hurd et al., 2003; Omori and Malicki, 2006; van de Pavert et al., 2007; Park et al., 2011; Flores-Benitez and Knust, 2015; Ramkumar et al., 2016). Functional interaction between Crb and Par complexes are well defined. MPP5a, one of the key components of the Crb complex, directly interacts with Par6 to recruit the Par complex and facilitates its aggregation at the apical domains of epithelial cells. On the other hand, aPKC phosphorylates the intracellular domain of Crb protein, resulting in the exchange of intracellular Crb partner from FERM-domain proteins to MPP5a, thus restricting the apical localization of Crb (Hurd et al., 2003; Sotillos et al., 2004; Penkert et al., 2004; Laprise et al., 2006; Hsu et al., 2006; Fletcher et al., 2012; Wei et al., 2015). Because of this functional association, the precise mechanism and exact function of both complexes during the

[1]Eye Center of the Second Affiliated Hospital, School of Medicine, Zhejiang University, Hangzhou 310058, China. [2]The Institute of Translational Medicine, Zhejiang University, Hangzhou 310058, China. [3]Life Sciences Institute and Innovation Center for Cell Signaling Network, Zhejiang University, Hangzhou 310058, China. [4]Department of Cell Biology, Neurobiology and Anatomy, Medical College of Wisconsin, Milwaukee, WI 53226, USA. [5]Zhejiang Provincial Key Lab of Ophthalmology, Hangzhou 310058, China.
*These authors contributed equally to this work

‡Authors for correspondence (jianzou@zju.edu.cn; xlren@zju.edu.cn)

Z.K., 0000-0003-3857-4299; P.X., 0000-0001-7726-5443; J.Z., 0000-0002-8884-9978

Handling Editor: Steve Wilson
Received 2 September 2019; Accepted 9 October 2020

Development (2020) 147, dev184457. doi:10.1242/dev.184457

remodeling of AJs is still inconclusive, although various phenotype defects of diverse organs have been reported upon their absence.

In this study, we aim to elucidate *in vivo* the coordinative mechanism linking epithelial membrane traffic, AJ remodeling and apical polarity machineries during cell state transition in vertebrates. Using the developing zebrafish lens and retina as models, we show that MPP5a interacts with GTPase Rab11 to transport both Crb complex and AJ components to the apical domain, thus establishing apical polarity. Dysfunction of either the Crb complex or Rab11 causes failure of the apical transport of Crb components and undesired and unstable punctum adherens, which leads to an invasive migration and cataract-like phenotype. On the other hand, the Par complex may regulate cytoskeleton arrangement to accommodate vesicle transport, but does not directly interact with Rab11.

RESULTS

AJs are dynamically remodeled during lens cell state transition

To investigate the mechanism of Crb complex involvement in AJ assembly, we first examined the wild-type (WT) zebrafish lens for the AJ remodeling pattern during cell state transition. E-cadherin displayed non-polarized localization in lens epidermal cells at 24 hpf (hours post fertilization) and was enriched at the vertex point where three neighbor cells meet (Fig. 1A,B). TEM observations revealed that tricellular adherens at the foci and punctum adherens between lateral membranes of epidermal cells was the major type of adhesion plaque in the lens (Fig. 1C,D; Fig. S1A-C). At 28 hpf, when epidermal-to-epithelial transition occurred (Greiling and Clark, 2009), E-cadherin gradually accumulated at the apical domains of

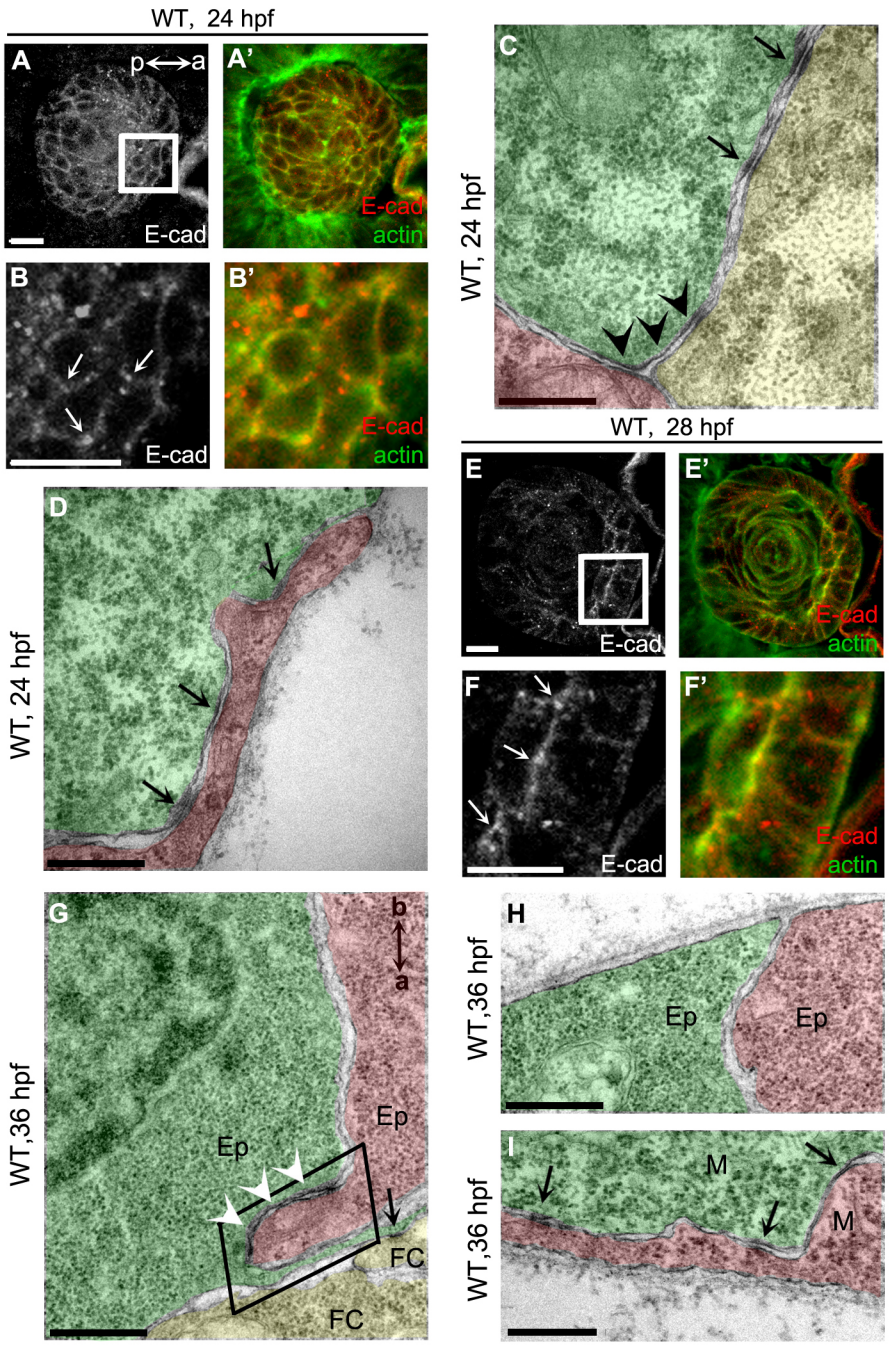

Fig. 1. AJs are dynamically remodeled during lens cell state transition. (A) E-cadherin was non-polarly distributed in lens epidermal cells at 24 hpf. (B) Higher magnification of the white boxed region in A. Arrows show the punctuated accumulation of E-cadherin at the vertex points where three neighbor epidermal cells meet. a (anterior) and p (posterior) indicate the lens orientation. (C,D) Tricellular adherens (C, black arrowheads) and lateral punctum adherens (D, arrows) were the major adhesion plaques between lens epidermal cells in WT at 24 hpf. Punctum adherens existed at the lateral (C) and basal (D) regions. (E) E-cadherin was enriched in the apical regions of epithelial cells when epidermal-to-epithelial transition occurred at 28 hpf. (F) Higher magnifications of the white boxed region in E. Arrows show the punctuated accumulation of E-cadherin in the apical regions of epithelial cells. (G) AJs were assembled into zonula adherens at the apical domain between epithelia (white arrowheads). a (apical) and b (basal) indicate the orientation of lens epithelial cells. The black boxed region shows the apical zone between two epithelial cells. (H) Few adhesion plaques were observed in the basal regions between epithelia in WT at 36 hpf. (I) Lateral punctum adherens, but not apical zonula adherens, were observed between mesenchymal cells when epithelial-to-mesenchymal transition occurred. Ep, epithelium; M, mesenchymal cells; FC, fiber cells. Lower magnification TEM images showing the position of C,D and G-I in lens are presented in Fig. S1. Scale bars: 10 µm (A,B,E,F), 400 nm (C,D,G-I).

Development (2020) 147, dev184457. doi:10.1242/dev.184457

epithelial cells in the anterior lens (Fig. 1E,F). TEM revealed that AJs were mainly rearranged into apical zonula adherens between the interface of two epithelial cells in mature lens epithelial cells at 36 hpf (Fig. 1G; Fig. S1D,E). In addition, we observed a few junction plaques at basal and lateral interfaces between epithelia at this stage (Fig. 1H; Fig. S1E). In the posterior lens, where epithelial cells were transformed into mesenchymal cells, the apical zonula adherens were disassembled and rearranged as lateral punctum adherens (Fig. 1I; Fig. S1F). These observations indicate that a dynamic transition of AJ assembly modes is required for lens development, as frequently observed in development of other organs (Nieto et al., 2016).

AJs components fail to accumulate at the apical domains of epithelial cells in *nok* mutants

We then examined the expression patterns of Crb protein and MPP5 in developing zebrafish lens. Among the isoforms of Crb and MPP5 in zebrafish (Omori and Malicki, 2006; Zou et al., 2010), only the isoforms Crb2a and Nok (Nagie oko, a MPP5a homolog in zebrafish) were significantly expressed in zebrafish lens epithelial cells (Fig. 2A-C; Fig. S2A-J). Coupling with the apical aggregation of E-cadherin, Crb2a and Nok were not expressed until epidermal-to-epithelial transition occurred (Fig. 2A,B; Fig. S2A,B). Similarly, we observed that the apical localization of Crb2a and Nok was

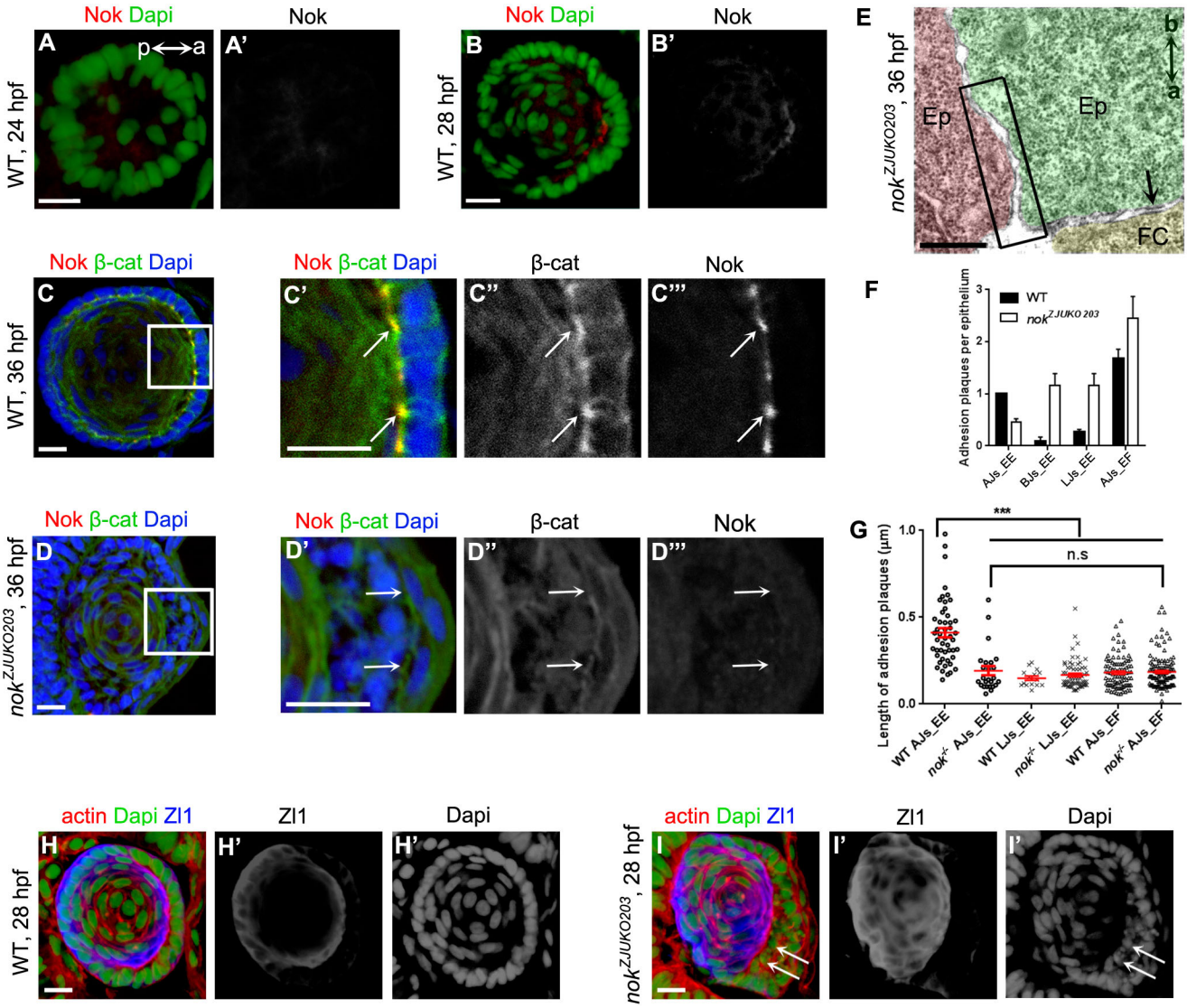

Fig. 2. AJ components fail to accumulate at the apical domains of epithelial cells in *nok* mutants. (A) Nok protein was not expressed in lens epidermal cells at 24 hpf. a (anterior) and p (posterior) show the lens orientation. (B) Nok started to be expressed in lens epithelial cells at 28 hpf when epidermal-to-epithelial transition occurred. (C,D) Apical enriched β-catenin colocalized with Nok in WT lens epithelial cells at 36 hpf. β-catenin lost its apical enrichment in *nok* mutants at 36 hpf. C′-C‴ and D′-D‴ are higher magnifications of the white boxed regions in C and D, respectively. (E) Apical zonula adherens disappeared in *nok* mutants at 36 hpf. a (apical) and b (basal) show the orientation of lens epithelial cells. (F) Quantification of the number of adhesion plaques in lens epithelial cells in WT and *nok* mutants at 36 hpf. In WT lens, the apical AJs between epithelia (AJs_EE, 1 per epithelium) and the apical AJs between epithelia and fiber cells (AJs_EF, 1.68 per epithelium) were the major types of adhesion plaques. In *nok* mutants, AJs_EE number significantly decreased (0.45 per epithelium) and the number of other types of adhesion plaques, including the basal AJs between epithelia (BJs_EE), the lateral AJs between epithelia (LJs_EE) and AJs_EF, significantly increased. (G) Quantification of the length of adhesion plaques in epithelial cells in WT and *nok* mutants at 36 hpf. The length of AJs_EE (0.41±0.03 μm) was significantly longer than LJs_EE (0.15±0.01 μm) and AJs_EF (0.18±0.01 μm) in WT. The length of AJs_EE in *nok* mutants (0.19±0.02 μm) was significantly reduced and comparable with LJs_EE and AJs_EF (*n*=49 epithelial cells for WT and 59 for *nok* mutants). (H,I) Compared with WT (H), a large number of Zl1-immunoreactive negative cells (arrows) accumulated in the inner lens in *nok* mutants at 28 hpf (I). Scale bars: 10 μm (A-D,H,I), 400 nm (E). ***P<0.001, n.s>0.05.

Development (2020) 147, dev184457. doi:10.1242/dev.184457

reciprocally dependent in lens epithelial cells (Fig. S2C,D). Thus, we further examined AJ assembly in *nok* (currently known as *mpp5a*) mutant zebrafish.

The point mutation or truncation of Nok with residual domains, such as nok^{m227} and nok^{m520} alleles, retains partial functions (Zou et al., 2013). To obtain clearer results, we generated a *nok* knockout fish line (named $nok^{ZJUKO203}$ in this study) using the CRISPR-Cas9 technique (Fig. S3A-D). The Nok protein in this line was truncated at amino acid 38, which is ahead of all conserved domains. A cataract-like phenotype developed in the *nok* mutant zebrafish (Fig. S3E,F). Immunostaining of β-catenin, which represents the distribution of AJs, revealed that dysfunction of Nok induced a loss of polarized AJ distribution in lens epithelial cells of *nok* mutants at 36 hpf (Fig. 2C,D). TEM revealed that AJ components failed to accumulate at apical domains to form zonula adherens (Fig. 2E). Statistical analysis indicated that AJs were substantially assembled into short punctum adherens and mainly distributed into the basal and lateral interfaces between epithelial cells and into the apical interfaces between epithelial and fiber cells, in sharp contradiction to those in WT lens (Fig. 2F). The increase in number of apical AJs between epithelial and fiber cells in *nok* mutants might be partially caused by invasion of epithelial cells into the inner lens. The average length of zonula adherens in WT lens epithelial cells was significantly longer than that of punctum adherens (Fig. 2G), implying a more stable lens epithelial structure stabilized by zonula adherens. The average length of all types of AJs in *nok* mutants was equivalent to that of punctum adherens, but significantly shorter than that of zonula adherens (Fig. 2G), suggesting that the stability of epithelial cells was affected. Indeed, we observed that epithelial cells directly invaded into the inner lens in *nok* mutants (Fig. S4A-E, Movies 1-4), resulting in its accumulation in the inner lens, which cannot be stained by the lens fiber cell marker Zl1 (Fig. 2H,I; Fig. S4C-E) (Imai et al., 2010). In contrast, epithelial cells were unable to migrate into the inner lens at this stage in the WT (Fig. S4A; Greiling and Clark, 2009). The loss of Nok did not affect the differentiation of lens fiber cells, as shown by Zl1 and Aqp0 staining in lens fiber cells (Fig. 2H,I; Fig. S5). At 36 hpf, the number of lens epithelial cells was lower in *nok* mutants than in the WT, whereas the number of lens fiber cells was higher in *nok* mutants than in the WT (Fig. S4F-H). The ingressed epithelial cells may progressively differentiate into lens fiber cells in *nok* mutants. Alternatively, the ingressed epithelial cells may be eliminated by cell death, and the denucleation of lens fiber cells may be delayed in *nok* mutants. As a result of this abnormal epithelial cells migration, *nok* mutant zebrafish developed a cataract-like phenotype. These data suggest that Nok is required for the proper assembly of AJs, which is important in cellular migration.

Apical localizations of Nok and Rab11 are reciprocally dependent

Given that Rab11 is crucial for guiding the vesicle trafficking of AJs, we speculated the existence of Crb complex-driven regulation of apically oriented trafficking of AJs molecules by Rab11-mediated exocytosis during epidermal-to-epithelial transition in the developing lens. We thus first examined the localization of Rab11. Intriguingly, Rab11 did not exhibit an apical enrichment in epidermal cells at 24 hpf (Fig. 3A), but strongly aggregated at the apical domains in mature epithelial cells where Crb2a was expressed at 36 hpf (Fig. 3B). In contrast, Rab11 lost its apical localization in *nok* mutants at 36 hpf (Fig. 3C). Consistently, both eGFP-tagged Rab11a proteins (eGFP-Rab11a) and its constitutive active mutation eGFP-Rab11a Q70L (Chen et al., 1998) were well enriched in apical regions in lens epithelial cells in WT zebrafish (Fig. 3D,E). However, in *nok* mutants, we observed that eGFP-Rab11 and eGFP-Rab11 Q70L were spread into the apical, lateral and basal regions at comparable eGFP intensity (Fig. 3F,G). The data suggest that the apical distribution of Rab11 requires accurate localization of the Crb complex.

To elucidate further, we generated $rab11a^{ZJUKO233}$ and $rab11ba^{ZJUKO234}$ knockout fish lines using the CRISPR-Cas9 technique, considering that Rab11a and Rab11ba are main isoforms in the zebrafish lens (Fig. S6) (Thisse et al., 2004). We observed that apical distribution of Crb2a required the activity of Rab11, as indicated by the finding that Crb2a partially lost its apical localization in lens epithelial cells in individual *rab11a* or *rab11ba* knockout mutants (Fig. 3H,I). Double knockout (dKO) mutants of *rab11a/rab11ba* completely lost this apical enrichment of Crb2a and Nok (Fig. 3J,K), suggesting the redundant function of Rab11a with Rab11ba in lens epithelial cells. Consistently, we observed that overexpression of Rab11a S25N, a dominant-negative Rab11 mutant (Chen et al., 1998), but not Rab11a, dose-dependently impeded the apical localization of Nok in WT lens epithelial cells (Fig. 3L-O). In detail, either sporadic overexpression generated by plasmid injection (Fig. 3D) or overall overexpression generated by injection of *Rab11a* mRNA (Fig. 3L) did not significantly affect the apical enrichment of Nok in WT lens epithelial cells. In contrast, lower level overexpression of Rab11a S25N induced the lateral and basal distribution of Nok (Fig. 3N), and higher level overexpression of Rab11 S25N significantly impeded the apical aggregation of Nok (Fig. 3M,O). Furthermore, in contrast to Rab11a, eGFP-tagged Rab11a S25N proteins spread to apical, lateral and basal regions at comparable eGFP intensity in WT lens epithelial cells (Fig. 3N). These observations show that the apical localizations of Nok and Rab11 are reciprocally dependent.

The reciprocal dependency between Rab11 and Crb complex was also observed in retinal neuroepithelial cells. Genetic ablation of one Rab11 isoform in retinal neuroepithelial cells weakened the apical distribution of Crb2a, whereas knockout of two Rab11 isoforms exaggerated this phenotype (Fig. S7A,B). In agreement with this observation, the Rab11a S25N mutant failed to enrich in the apical regions in WT retinal neuroepithelia, and eGFP-Rab11a also lost apical enrichment in *nok* mutants (Fig. S7C-H).

Rab11 plays crucial roles in both exocytosis and endocytosis, and Rab5 plays key roles in endocytosis (Stenmark, 2009; Scott et al., 2014; Woichansky et al., 2016). We therefore examined whether the endocytosis pathway was involved in the establishment of polarity in lens epithelial cells by overexpressing Rab5 S36N, a dominant negative form of Rab5 (Stenmark et al., 1994), in zebrafish embryos. In contrast to the overexpression of Rab11a S25N, we observed that the sporadic overexpression of Rab5 S36N did not affect the apical localization of Nok in WT lens epithelial cells (Fig. 3P), suggesting that endocytosis is not involved in Nok localization in lens epithelial cells. Interestingly, we observed that Nok proteins were ectopically present in fiber cells in the WT lens overexpressing either Rab5 S36N or Rab11a S25N (Fig. 3K-P), suggesting that endocytosis has an important role in breaking down the apical polarity in lens mesenchymal and fiber cells during epithelial-to-mesenchymal and fiber cell transition. These data suggest that the Crb complex guides apically oriented vesicle exocytosis mediated by Rab11 in epithelial cells of different origin.

MPP5a physically associates with Rab11 to promote their reciprocal apical localization

Given the reciprocal dependency between Rab11 and Crb complex, we speculated that component(s) of the Crb complex directly

Development (2020) 147, dev184457. doi:10.1242/dev.184457

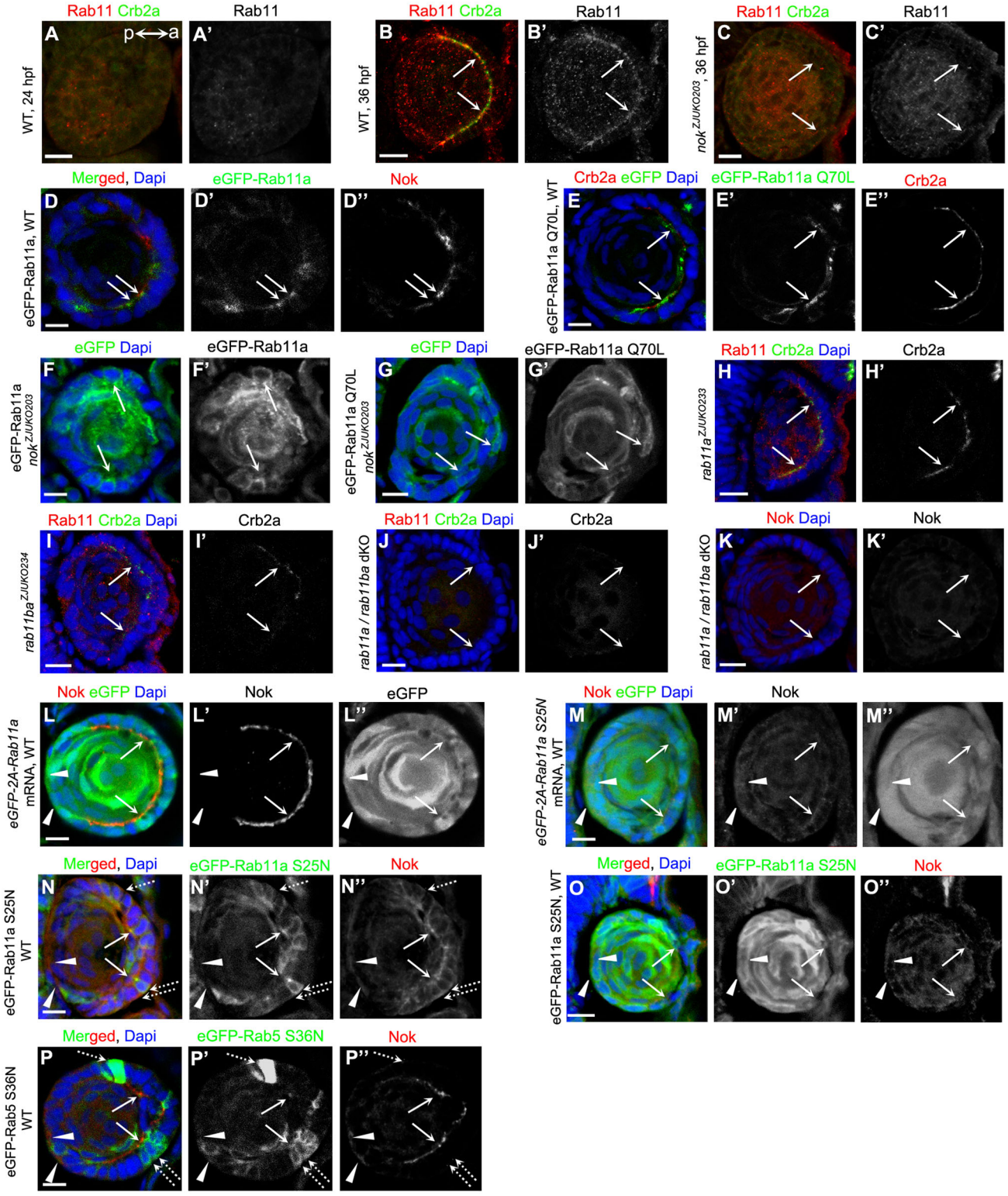

Fig. 3. See next page for legend.

interact with Rab11 to guide the orientated exocytosis of AJ molecules. We therefore inspected the interaction between Rab11 and a variety of polarity proteins using co-immunoprecipitation assays. As expected, Nok, but not the other polarity proteins examined, strongly interacted with Rab11a (Fig. 4A), even though the Par complex and Par5 are reported to be involved in Rab11-mediated vesicle exocytosis (Bryant et al., 2010; Winter et al., 2012). Domain mapping analysis revealed that the L27-PDZ-SH3 domain (amino acids 151-505) of Nok was necessary and sufficient for Rab11a interaction (Fig. 4B). Surprisingly, Rab11a S25N, the dominant negative mutant of Rab11, was unable to interact with Nok, whereas the constitutive active Rab11a (Q70L) exhibited a stronger Nok interaction (Fig. 4C). Importantly, in MDCK cells, a widely used *in vitro* model for studies of polarization (Simmons,

Development (2020) 147, dev184457. doi:10.1242/dev.184457

Fig. 3. The apical localizations of Nok and Rab11 are reciprocally dependent. (A,B) Temporospatial expression pattern of Rab11 in zebrafish lens. Rab11 did not display polarized aggregation in epidermal cells when Crb2a was not detectable at 24 hpf (A), but strongly aggregated in the apical regions in lens epithelial cells at 36 hpf (B). a (anterior) and p (posterior) show the lens orientation. (C) Rab11 lost its apical enrichment in lens epithelial cells in *nok* mutants. (D,E) eGFP-tagged Rab11a (D) and Rab11 Q70L (E) proteins were enriched in the apical regions in lens epithelial cells in WT. Overexpression of eGFP-Rab11a and eGFP-Rab11 Q70L did not significantly affect the apical enrichment of Nok. (F,G) eGFP-tagged Rab11a (F) and Rab11 Q70L (G) proteins were distributed at the lateral and basal regions in lens epithelial cells in *nok* mutants. (H-K) The apical localization of Crb2a in lens epithelial cells was partially disrupted in *rab11a* (H) or *rab11ba* mutants (I) and completely disrupted in *rab11a*/*rab11ba* dKO mutants (J). Similarly, the apical localization of Nok was lost in *rab11a*/*rab11ba* dKO mutants (K). (L,M) Overexpression of eGFP-2A-Rab11a (L) or eGFP-2A-Rab11a S25N (M) following mRNA injection. Overexpression of Rab11a S25N (M), but not Rab11a (L), impeded the apical aggregation of Nok. Low levels of Nok were observed in mesenchymal cells overexpressing eGFP-2A-Rab11a S25N in the posterior lens (M, white triangles). (N,O) eGFP-Rab11a S25N is evenly spread to apical, lateral and basal regions in WT lens epithelial cells. Lower level overexpression of eGFP-Rab11a S25N induced the lateral and basal distribution of Nok (N), and higher level of eGFP-Rab11a S25N impeded the apical aggregation of Nok (O). Low levels of Nok were observed in mesenchymal cells overexpressing eGFP-Rab11a S25N in the posterior lens (white triangles). (P) Overexpression of eGFP-Rab5 S36N did not significantly affect the apical enrichment of Nok in WT lens epithelial cells. Low levels of Nok (white triangles) were observed in mesenchymal cells overexpressing eGFP-Rab5 S36N in the posterior lens. The embryos used for B-P were fixed at 36 hpf. Arrows show the apical regions of lens epithelial cells. Broken arrows show the basal regions of lens epithelial cells. White triangles show fiber cells in the posterior lens. Plasmids pTol2-*EF1*::eGFP-Rab11a, pTol2-*EF1*::eGFP-Rab11a S25N, pTol2-*EF1*::eGFP-Rab11a Q70L or pTol2-*EF1*::eGFP-Rab5 S36N were used for the sporadic overexpression of eGFP-tagged Rab proteins shown in Fig. 3D-G,N-P. Scale bars: 10 µm.

1982; Chavrier et al., 1990), we observed that Rab11 formed an endogenous complex with Pals1 (MPP5a homolog in mammals), but not the other tested polarity proteins (Fig. 4D). The co-immunoprecipitation results using zebrafish eye extracts further confirmed that Rab11 interacted with Nok in zebrafish (Fig. 4E). The data suggest that a complex is formed by Nok and Rab11, which could determine the function of Rab11 in vesicle exocytosis.

We then investigated whether the Crb and Par complexes affect the cellular distribution of AJs in HEK293T cells. We observed that co-expression of Crb2a and Nok induced a significant increase in membrane association of β-catenin compared with neighbor control cells, which were transfection negative (Fig. 4G,K). In contrast, the expression of eGFP did not affect the expression and localization of β-catenin (Fig. 4F,K), and the expression of aPKCλ and Pard6 increased the level of cytoplasmic β-catenin but did not significantly induce its membrane-associated distribution (Fig. 4H,K). As expected, expression of Rab11a S25N, but not Rab11a, substantially impeded the phenotype driven by co-expression of Crb2a and Nok (Fig. 4I-K). Furthermore, we observed that eGFP-Rab11a, Nok-mCherry and eGFP-Rab11a S25N were spread throughout the whole cell without aggregation when these proteins were individually expressed in MDCK cells (Fig. S8A-C). However, eGFP-Rab11a and Nok-mCherry were aggregated into dot-like foci when these two proteins were co-expressed (Fig. 4L-P). As the control, the co-expression of eGFP-Rab11a S25N and Nok-mCherry did not display a similar phenotype (Fig. S8D). We observed that about 29% of eGFP-Rab11a foci and 41% of Nok-mCherry foci were colocalized in Golgi but not in endoplasmic reticulum (Fig. 4N). These data indicate that the Nok-Rab11 complex is formed mainly in Golgi. These results suggest that Nok, rather than other polarity proteins, forms a previously unrecognized complex with Rab11 to orientate the exocytosis of AJ components.

Rab11 determines the localization and assembly of AJs

We then investigated whether Rab11 dysfunction phenocopies the AJ remolding defects, similarly to Crb complex dysfunction. We observed a compromised β-catenin aggregation at the apical domains in lens epithelial cells of *rab11a*^{ZJUKO233} or *rab11ba*^{ZJUKO234} mutants, which was further exaggerated when both were ablated (Fig. 5A-H). As with dysfunction of the Crb complex, double ablation of *rab11a* and *rab11ba* prevented formation of zonula adherens (Fig. 5I,K-M). Interestingly, the number of apical punctum adherens between lens epithelial cells and fiber cells was significantly reduced in *rab11a/rab11ba* dKO mutants (Fig. 5K), suggesting an important role of Rab11 in the formation of apical AJs between epithelial and fiber cells (AJs_EF). Single *rab11a* or *rab11ba* knockout partially affected the number and average length of apical AJs between epithelia (AJs_EE), but did not induce a significant change in AJs_EF (Fig. 5K,L), probably because of the redundant function of these two proteins. More AJ molecules appeared to be transported into the lateral regions to form punctum adherens (Fig. 5K,M). Consistent with these observations, Rab11a S25N disrupted the apical enrichment of β-catenin (Fig. 5E,F) and the proper AJ remodeling during epidermal-to-epithelial transition, a phenotype similar to *rab11a/rab11ba* dKO or the dysfunction of Nok (Fig. 5J-M). The data suggest that Rab11-mediated transportation of AJ molecules enters into apical regions, both between epithelia and between epithelial and fiber cells and not just to the limited apical domains between epithelial cells as previously known.

Apical localization of aPKC is not associated with Rab11

Par complex is also known to be involved in apical zonula adherens formation in epithelial cells (Joberty et al., 2000). Intriguingly, our data indicate that key components of the Par complex, including aPKCλ, Pard6 and Pard3, failed to interact with Rab11 (Fig. 4A), implying a distinct mechanism of Par complex participation in AJ remodeling. Immunostaining of aPKC showed a much earlier and more extensive expression pattern than seen for the components of Crb complex (Fig. 6A-C). In particular, aPKC was expressed but only enriched at the apical domains when Crb2a was expressed and epidermal-to-epithelial transition had started (Fig. 6A,B). In contrast to the restrictive expression of Crb2a in epithelia, aPKC was also expressed in mesenchymal and primary fiber cells and displayed a non-polarized distribution (Fig. 6C). We observed that aPKCλ ablation resulted in the disappearance of apical zonula adherens in mature lens epithelial cells (Fig. 6D). Intriguingly, phenotypes of *aPKCλ* mutants in AJ remodeling appeared to be associated with expression of the Crb complex, as ablation of aPKCλ exhibited no significant phenotype in lens epidermal cells or in surface epidermal cells where Crb complex is absent (Fig. 6E).

To elucidate whether the apical localizations of aPKC and Rab11 are reciprocally dependent, we examined the localization of Crb2a, Rab11, aPKC and F-actin in *aPKCλ*, *rab11a/rab11ba* and *nok* mutants. In *aPKCλ*^{m567} mutants, the immunostaining signal of aPKC was lost, and actin also lost its apical enrichment (Fig. 6F). Interestingly, we frequently observed a heterogeneity for the localization of Crb2a and Rab11 in lens epithelial cells in *aPKCλ* mutants. Specifically, both Crb2a and Rab11 lost their apical localization in most lens epithelial cells (63%, n=167 cells in 10 retinas) in *aPKCλ* mutants. However, Rab11a was colocalized with Crb2a in the lens epithelial cells in which Crb2a was localized at the apical domains (Fig. 6G). In *rab11a/rab11ba* dKO mutants, immunohistochemistry results clearly showed that Rab11, Crb2a

Development (2020) 147, dev184457. doi:10.1242/dev.184457

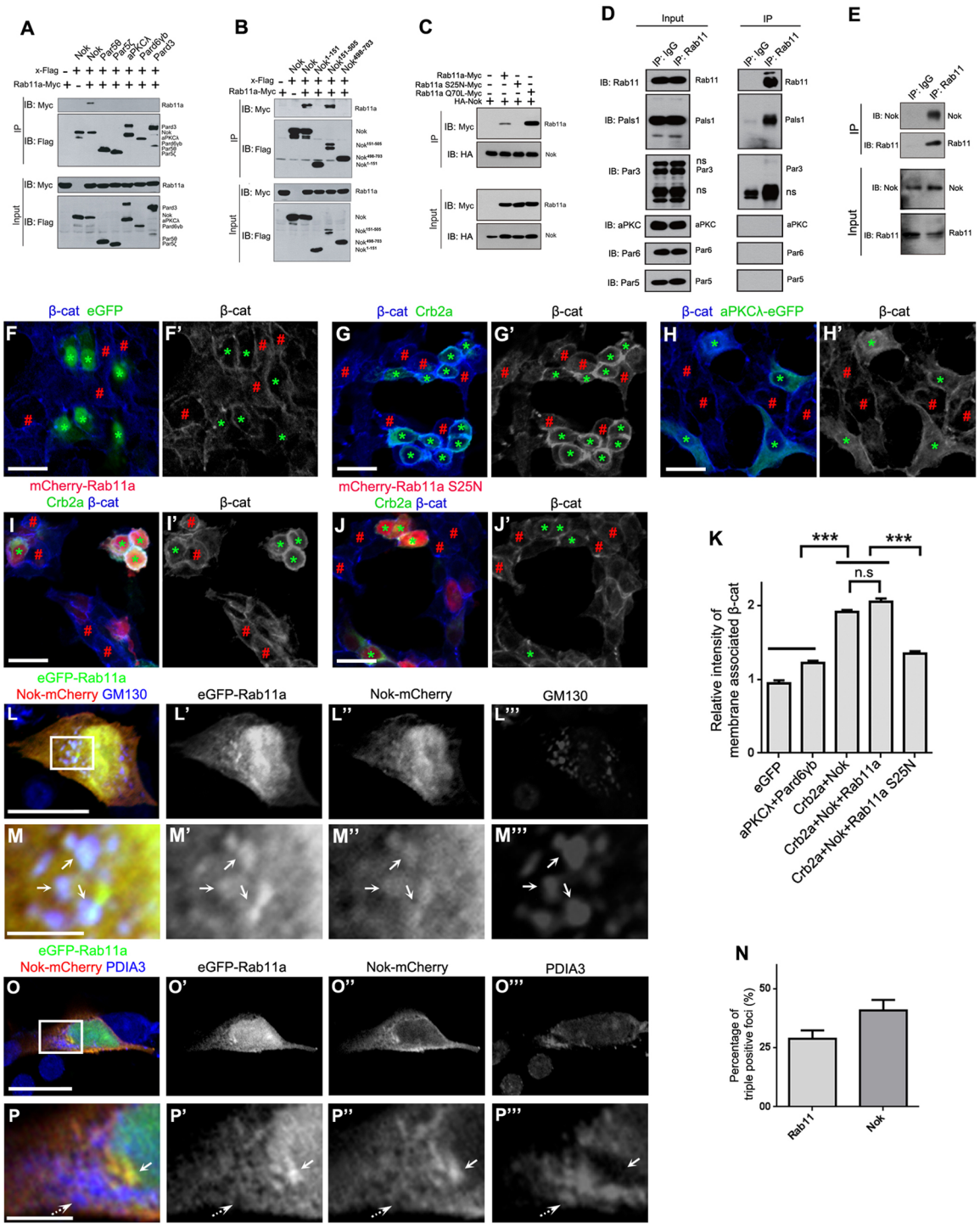

Fig. 4. Nok interplays with Rab11 to promote membrane association of β-catenin in human cultured cells. (A) Nok, but not the other polarity proteins examined, including Par5θ, Par5ζ, aPKCλ, Pard6γb and Pard3, interacted with Rab11a. (B) The L27-SH3-PDZ domain of Nok (Nok$^{151-505}$) interacted with Rab11a. (C) The dominant negative Rab11a (S25N) did not interact with Nok, although the constitutively active Rab11a (Q70L) had a higher affinity for Nok than wild-type Rab11a. (D) Co-immunoprecipitation verified the endogenous complex between Rab11 and Nok in MDCK cells, but not the other tested proteins. (E) Co-immunoprecipitation using zebrafish eye extracts verified the endogenous complex between Nok and Rab11 in zebrafish. (F-H) Co-expression of Crb2a and Nok (G), but not co-expression of aPKCλ and Pard6γb (H) or expression of eGFP (F) promoted the membrane association of β-catenin in HEK293T cells. Green asterisks indicate transfection-positive cells and red # symbols indicate transfection-negative neighbor cells. (I,J) The expression of Rab11a S25N (J), but not Rab11a (I) impeded the membrane association of β-catenin induced by co-expression of Crb2a and Nok in HEK293T cells. (K) Quantification of fluorescence intensity of membrane-associated β-catenin shown in F-J (n>60 cells). Relative intensity was calculated by dividing the intensity in cells marked by an * by that in cells marked by a # symbol. (L-P) eGFP-Rab11a was colocalized with Nok-mCherry in Golgi (L,M; labeled by GM130), but not in endoplasmic reticulum (O,P; labeled by PDIA3) in MDCK cells. M and P are higher magnifications of the white boxed regions in L and O, respectively. Arrows show the aggregation of eGFP-Rab11a and Nok-mCherry, broken arrows show endoplasmic reticulum. (N) Quantification of the percentage of triple positive foci in Rab11a-positive foci and Nok-positive foci shown in L (n>60 cells). Scale bars: 20 µm (F-J), 10 µm (L,O), 2.5 µm (M,P). ***P<0.001, n.s>0.05.

Development (2020) 147, dev184457. doi:10.1242/dev.184457

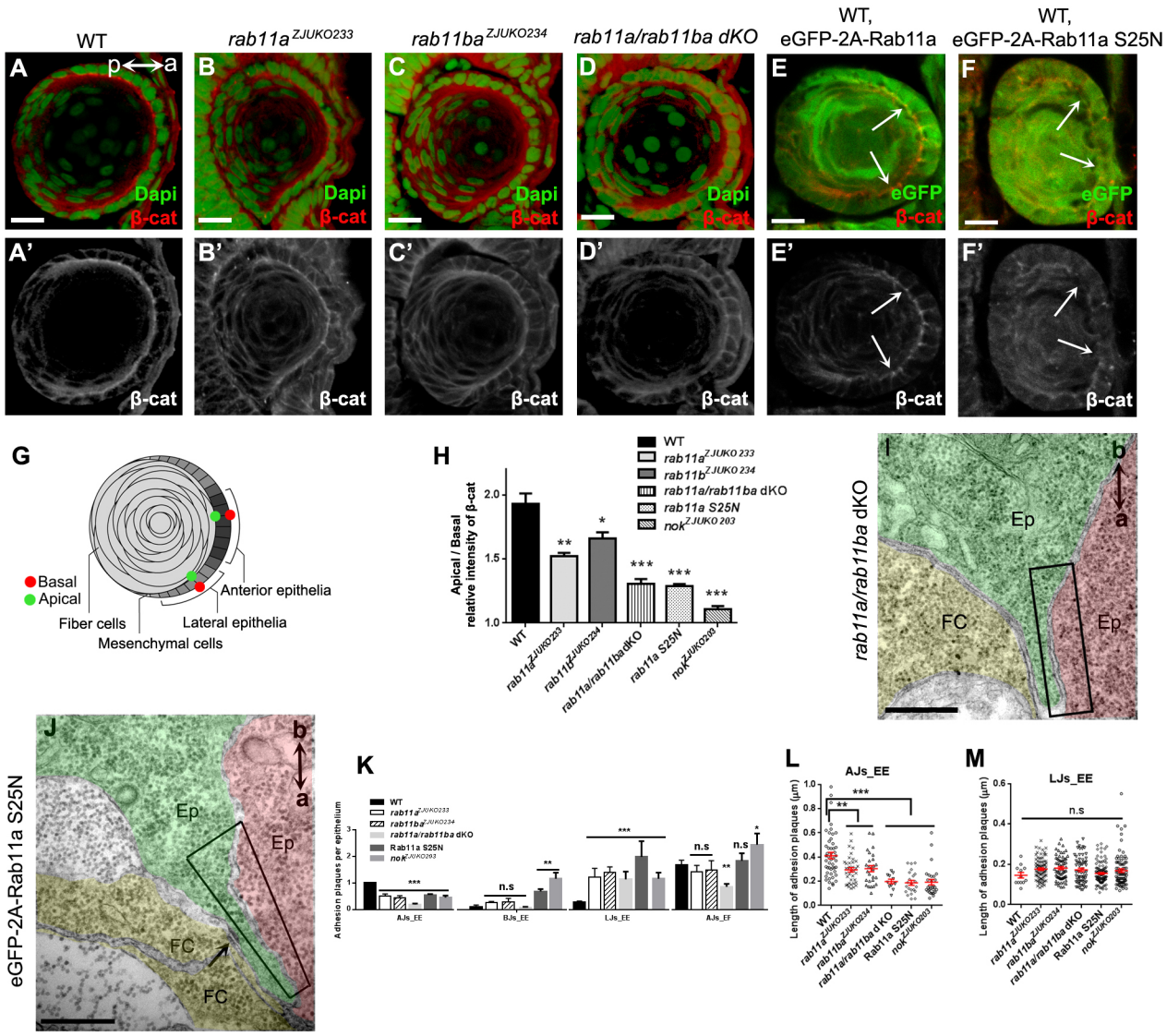

Fig. 5. Rab11 determines the localization and assembly of AJs. (A-F) The distribution of β-catenin in WT (A), *rab11a* (B), *rab11ba* (C), *rab11a*/*rab11ba* dKO (D), eGFP-2A-Rab11a overexpressed (E) and eGFP-2A-Rab11a S25N overexpressed (F) embryos at 36 hpf. a (anterior) and p (posterior) in A show the lens orientation. Arrows (E,F) show that eGFP-2A-Rab11a S25N, but not eGFP-2A-Rab11a, impeded the apical enrichment of β-catenin. (G) Scheme showing locations of apical and basal spots for relative fluorescence intensity measurements. (H) Quantification of apical/basal relative intensity of β-catenin shown in A-F (*n*=20 lenses from 10 embryos). (I,J) Both dKO of *rab11a*/*rab11ba* (I) and overexpression of Rab11a S25N (J) disrupted the AJs_EE zonula adherens at 36 hpf. Arrow shows AJs_EF punctum adherens. a (apical) and b (basal) show the orientation of lens epithelial cells. (K) Overexpression of Rab11a S25N or *rab11a*/*rab11ba* dKO significantly impeded the formation of AJs_EE. The number of AJs_EF also significantly decreased in *rab11a*/*rab11ba* dKO mutants (*n*=56 epithelial cells for *rab11a*/*rab11ba* dKO mutants, and 73 for Rab11a S25N overexpressed embryos). (L) The length of AJs_EE in Rab11a S25N overexpressed or *rab11a*/*rab11ba* dKO mutant lens (0.19±0.02 μm) was comparable with that in *nok* mutants and significantly shorter than that in WT. (M) Although the number of LJs_EE significantly increased in Rab11a S25N overexpressed or *rab11a*/*rab11ba* dKO mutant lens (0.15±0.01 μm), the length of LJs_EE was comparable with that in WT and *nok* mutants. Ep, epithelium; FC, fiber cells. Scale bars: 10 μm (A-F), 400 nm (I,J). **P*<0.05, ***P*<0.01, ****P*<0.001, n.s>0.05.

and Nok were all lost in lens epithelial cells (Fig. 3J,K; Fig. 6H,I). However, both aPKC and actin were nicely enriched at the apical regions (Fig. 6H,I). In *nok* mutants, we also frequently observed a heterogeneity for the apical localization of aPKC between anterior and lateral lens epithelial cells. The immunostaining signals showed that both Crb2a and Rab11 concurrently lost their apical enrichment in lateral lens epithelial cells in *nok* mutants (Fig. 3C). However, aPKC and F-actin still displayed apical enrichment in lateral lens epithelial cells in *nok* mutants (Fig. 6J,K). The mechanism through which the heterogeneity is induced remains largely unknown, although some proteins (such as Pak1) probably have redundant functions (Aguilar-Aragon et al., 2018). Together with the observations on the localization of Crb2a, Rab11, aPKC, and F-actin in WT and mutants, the fact that Nok interacts with Rab11 leads to the conclusion that the apical localization of aPKC is not associated with Rab11, in contrast to the Crb-MPP5a complex.

Cytoskeletal modulation is also involved in vesicle trafficking (Lanzetti, 2007; Horgan and McCaffrey, 2011). The dynamic assembly of the Par complex is known to regulate actin and microtubule cytoskeleton organization (Überall et al., 1999; Betschinger et al., 2003; Harris and Peifer, 2007), and aPKC modulates the orientation of actomyosin cables to facilitate Rab11-mediated exocytosis in the *Drosophila* airway tubes (Hosono et al., 2015). Consistent with these reports, we observed that the apical

Development (2020) 147, dev184457. doi:10.1242/dev.184457

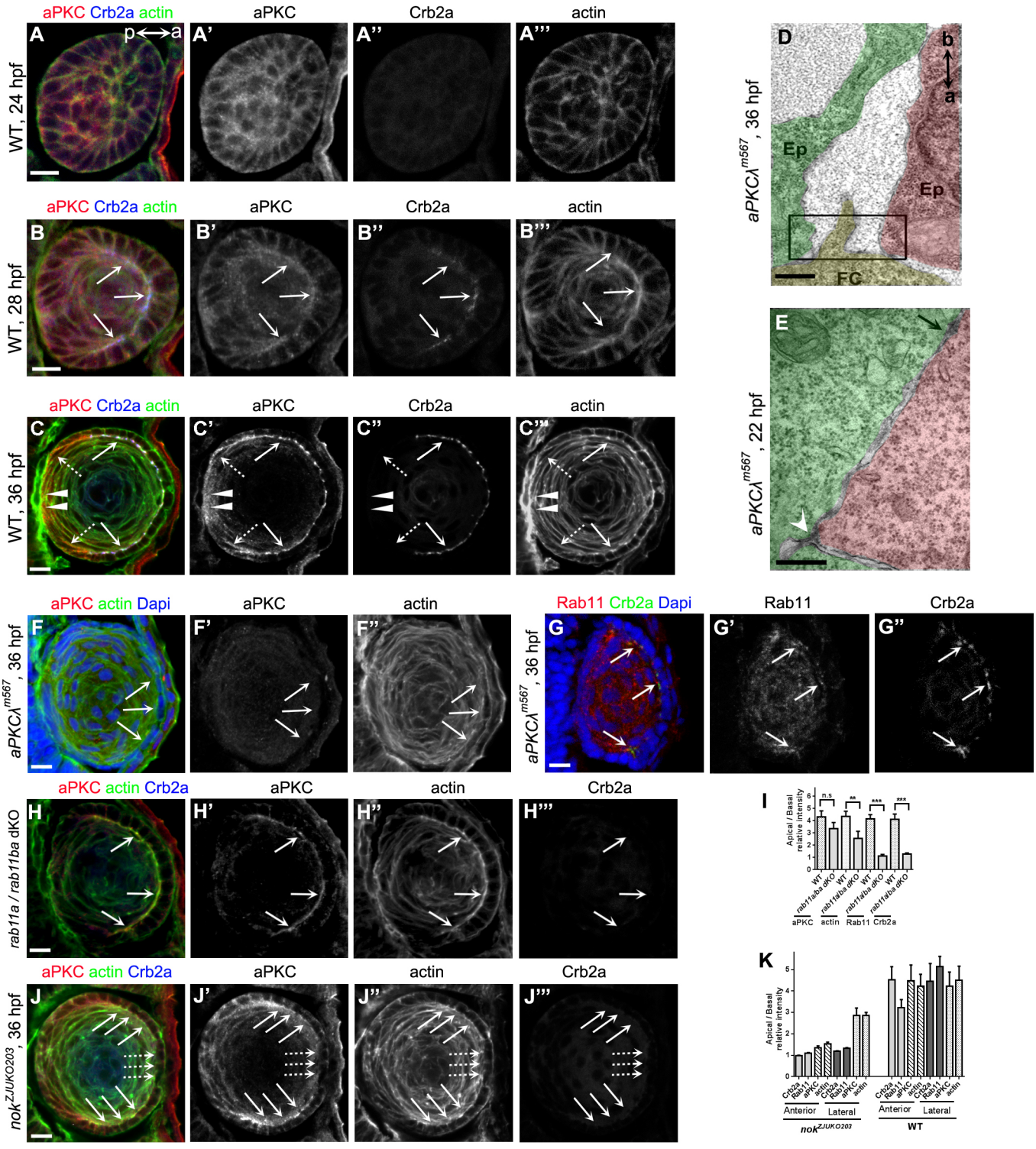

Fig. 6. See next page for legend.

enrichment of F-actin was closely associated with aPKC localization in lens epithelia, rather than localization of Crb complex (Fig. 6F-H,J). Taken together, these data imply that aPKC affects AJ remodeling through cytoskeleton modulation.

DISCUSSION

The cell state and the type of AJ can be accurately identified, which makes the developing vertebrate lens an ideal model for investigating the cell state transition and AJ remodeling *in vivo*. Using this model, we propose a molecular model whereby Crb and Par complexes are synergized to promote the Rab11-mediated remodeling of AJs. Crb and Par complexes are known to play conserved roles in modulating cell behaviors in many organs derived from epithelia from *Drosophila* to mammals (Tepass, 2012; Chen and Zhang, 2013; Campanale et al., 2017). Our data indicate that the apical localization of Crb complex is associated with Rab11

Development (2020) 147, dev184457. doi:10.1242/dev.184457

Fig. 6. aPKC organizes cytoskeleton to promote AJ remodeling, but apical localization of aPKC does not require Rab11. (A-C) Temporospatial expression pattern of aPKC in zebrafish lens. (A) aPKC displays non-polarized distribution in lens epidermal cells when Crb2a was not expressed at 24 hpf. (B) Coupling with Crb2a expression in epithelia, aPKC was accumulated to the apical domains at 28 hpf. (C) aPKC was restricted at the apical domains and colocalized with Crb2a in epithelial cells at 36 hpf. In contrast to Crb2a, aPKC was also expressed in lens mesenchymal cells (broken arrows) and primary fiber cells (arrowheads). Arrows show the apical aggregation of aPKC, Crb2a and actin in lens epithelial cells. Broken arrows show the lens mesenchymal cells. Arrowheads show the primary fiber cells. a (anterior) and p (posterior) in panel A show the lens orientation. (D) Apical zonula adherens disappeared in lens epithelial cells in *aPKCλ* mutants at 36 hpf. a (apical) and b (basal) show the orientation of lens epithelial cells. The black boxed region in D shows the apical zone between two epithelial cells. (E) Tricellular adherens (white arrowhead) and lateral punctum adherens (black arrow) between lens epidermal cells in *aPKCλ* mutants at 22 hpf. (F) In *aPKCλ* mutants, aPKC staining had disappeared (F), actin lost its apical enrichment. Arrows show the apical regions of lens epithelial cells. (G) In *aPKCλ* mutants, Crb2a and Rab11 lost their apical distribution in most epithelial cells at 36 hpf. Arrows show the apical colocalization of Crb2a and Rab11. (H) In *rab11a*/*rab11ba* dKO mutants, Crb2a lost its apical aggregation at 36 hpf. In contrast, aPKC and actin were still enriched at the apical domains in lens epithelial cells. Arrows show the apical regions of lens epithelial cells. (I) Quantification of apical/basal relative fluorescence intensity of aPKC, actin, Crb2a and Rab11 in WT and *rab11a*/*rab11ba* dKO mutants shown in H. aPKC displayed normal apical enrichment in *rab11a*/*rab11ba* dKO mutant lens epithelial cells; however, apical enrichment of actin, Crb2a and Rab11 was significantly decreased although actin reduction was mild (*n*=20 lenses from 10 embryos). (J) The apical localization of aPKC and actin displayed a heterogeneity in different lens epithelial cells in *nok* mutants at 36 hpf. Broken arrows show that aPKC and actin lost their apical enrichment in the anterior epithelial cells. Arrows show that aPKC and actin were still enriched in the apical regions in lateral epithelial cells. (K) Quantification of apical/basal relative fluorescence intensity of aPKC, actin, Crb2a and Rab11 in *nok* mutants shown in J and Fig. 3C. The apical enrichment of actin was associated with aPKC, whereas the apical enrichment of Rab11 was associated with Crb2a. Crb2a and aPKC showed concurrent apical localization in anterior epithelia, but not in lateral epithelial cells (*n*=20 lenses from 10 embryos). Scale bars: 10 µm (A-C,F-I), 400 nm (D,E). ***P*<0.01, ****P*<0.001.

in a dose-dependent manner. Loss of a single *rab11* isoform partially disrupts the apical localization of Crb complex and AJ remodeling in epithelia, whereas loss of more *rab11* isoforms leads to a more severe phenotype. The association between Rab11 and the Crb complex occurs in both mature lens epithelial cells and retinal neuroepithelial cells. The presence of slight apical enrichment of Crb2a in retinal neuroepithelial cells (Fig. S7A,B) might be caused by the redundant functions of other *rab11* isoforms, such as *rab11bb* (Thisse and Thisse, 2004). The model proposed in this study for coordination of AJ remodeling and cell migration pattern may also apply to other epithelia-derived tissues.

Because of their functional association, ablation of Rab11, the Crb complex or the Par complex leads to similar defects in AJ modeling in epithelial cells. However, we illustrate here that distinct complexes each play a specific role in organizing AJ remodeling. The Crb complex orientates the AJs_EE vesicle traffic of AJ molecules and stabilizes them into zonula adherens through the direct interplay between MPP5a and Rab11. One possibility is that the dysfunction of Crb complex leads to stochastic orientation of Rab11-mediated vesicle traffic to the apical interface between epithelial and fiber cells (AJs_EF) and the lateral interface between epithelia (LJs_EE).

In contrast to the epithelial-specific expression of Crb complex, the Par complex is also expressed in epidermal cells, mesenchymal cells and tumor cells (Fig. 6) (Halaoui and McCaffrey, 2015). The expression of Par complex in mesenchymal cells and tumor cells cannot induce the formation of apical zonula adherens, which also suggests that the disappearance of zonula adherens caused by aPKC dysfunction is mediated indirectly through the Crb complex. Thus, we speculate that, by stabilizing the apical membrane localization of Crb complex and by modulating the cytoskeleton to facilitate Rab11-mediated vesicle exocytosis, the Par complex promotes formation of apical polarity and zonula adherens in epithelial cells. When the Crb complex and adherens components are transported to the apical domains in epithelia, aPKC may separate AJs from the Crb complex via phosphorylation of Crb and Par3, thus defining the apical-lateral border (Sotillos et al., 2004; Morais-de-Sá et al., 2010; Wei et al., 2015).

Both endocytosis and exocytosis pathways play important roles in the remodeling of AJs (Stenmark, 2009; Scott et al., 2014; Woichansky et al., 2016). In this study, we observed that the dysfunction of Rab5, a key regulator of early endosome formation (Chavrier et al., 1990; Gorvel et al., 1991; Barbieri et al., 1996), did not affect the apical localization of Nok, suggesting that the endocytosis pathway is not involved in polarity formation in lens epithelial cells. During the epidermal-to-epithelial transition of lens cells, we observed that most AJs were converted from tricellular adherens and punctum adherens in lens epidermal cells to AJs_EE (zonula adherens) and AJs_EF (punctum adherens) in lens epithelial cells (Fig. 2F). In *rab11a/rab11ba* dKO mutants, both the AJs_EE and the AJs_EF in lens epithelial cells significantly decreased (Fig. 5K), suggesting an important role of Rab11 in the formation of these apical AJs. Given that Rab11 plays roles in both endocytosis and exocytosis pathways (Ullrich et al., 1996; Chen et al., 1998; Woichansky et al., 2016), the precise role of endocytosis and exocytosis in the formation of AJs_EE and AJs_EF remains to be elucidated in future studies.

In summary, our data identify a novel MPP5a-Rab11 complex. The interplay between Nok and Rab11 synergistically establishes apical polarity as well as the formation of zonula adherens during maturation of epithelial cells, probably through regulation of apical exocytosis.

MATERIALS AND METHODS

Zebrafish strains

Zebrafish were bred and maintained in accordance with Zhejiang University Animal Care and Use Committee protocols. AB WT, $crb2a^{m289}$ (Omori and Malicki, 2006), $aPKC\lambda^{m567}$ (Horne-Badovinac et al., 2001), $nok^{ZJUKO203}$ (this study), $rab11a^{ZJUKO233}$ (this study) and $rab11a^{ZJUKO234}$ (this study) were used in this study. Embryos were collected and kept in E3 embryo buffer (5 mM NaCl, 0.17 mM KCl, 0.33 mM $CaCl_2$ and 0.33 mM $MgSO_4$). Embryos were grown at 28°C in an incubator.

Generation of knockout zebrafish using CRISPR-Cas9

Single guide (sg)RNAs (final concentration 25-50 pg per embryo) targeting *nok, rab11a* and *rab11ba* genes and *Cas9* mRNA (final concentration 50-100 pg per embryo) were co-injected into AB WT zebrafish embryos at the one-cell stage. Founder fish were raised to adulthood and outcrossed with AB WT fish to obtain F1 generation. The generated knockout lines were named $nok^{ZJUKO203}$, $rab11a^{ZJUKO233}$ and $rab11a^{ZJUKO234}$ in this study. Heterozygous F1 adult zebrafish were outcrossed with AB WT fish to obtain F2 generation. Heterozygous F2 fish were incrossed to obtain homozygous mutant embryos for the analyses. Oligonucleotide sequences used for generating and genotyping the zebrafish knockout lines are listed in Table S1.

In vitro transcription of RNA and micro-injection

RNAs were transcripted *in vitro* using the mMESSAGE mMACHINE kit (Thermo Fisher Scientific, AM1344). For mRNA injection, we injected 50-100 pg mRNA into AB WT embryos at the one-cell stage. For plasmid injection, as much as 25 pg of plasmid along with 50 pg of *Tol2 transposase* mRNA was co-injected into zebrafish embryos. To examine the effects of overexpression of Rab11 or Rab5, we generated plasmids pTol2-*EF1*::eGFP-

Development (2020) 147, dev184457. doi:10.1242/dev.184457

Rab11a, pTol2-*EF1*::eGFP-Rab11a S25N, pTol2-*EF1*::eGFP-Rab11a Q70L and pTol2-*EF1*::eGFP-Rab5 S36N (Clark et al., 2011). For the sporadic overexpression of N-terminal eGFP-tagged Rab proteins shown in Fig. 3D-G,N-P, we injected the plasmids pTol2-*EF1*::eGFP-Rab11a, pTol2-*EF1*:: eGFP-Rab11a S25N, pTol2-*EF1*::eGFP-Rab11a Q70L or pTol2-*EF1*:: eGFP-Rab5 S36N together with *Tol2 transposase* mRNA into zebrafish embryos. For the mRNA overexpression shown in Fig. 3L,M and Fig. 5E,F, we generated plasmids pCS2-eGFP-2A-Rab11a and pCS2-eGFP-2A-Rab11a S25N, adding 2A peptide between eGFP and Rab11a by overlapping PCR based on the above constructs. Peptide 2A could self-cleave the proteins eGFP-2A-Rab11 and eGFP-2A-Rab11-S25N to release free eGFP (as the expression marker) and target proteins to avoid mutual interference between eGFP and the target proteins. We injected mRNAs encoding eGFP-2A-Rab11a and eGFP-2A-Rab11a S25N into zebrafish embryos.

Time-lapse imaging

The plasmid *pTol2-H2A::eGFP* was injected into WT and $nok^{ZJUKO203}$ embryos at the one-cell stage to mosaically label lens cells. At 28 hpf, the embryos expressing eGFP in the lens were mounted in 1% low-melting-point agarose in E3 embryo medium with 168 mg/l tricaine for anesthetization in a glass-bottom FluoroDish (World Precision Instrument). Embryos were imaged using 10× dipping objectives on a Nikon A1 confocal microscope. The lens epithelial cells labeled with eGFP were imaged every 10 or 30 min after 28 hpf. The time-lapse imaging lasted 2 h from 28 hpf to 30 hpf.

Immunohistochemistry and antibodies

The following antibodies were used: anti-Aqp0 (1:200; Millipore AB3071), anti-Zl1 (1:200; Abcam ab185979), anti-β-catenin (1:200; Sigma C7207), anti-E-cadherin (1:100; BD transduction 610182; Arora et al., 2020), anti-ZO1 (1:200; Invitrogen 339100), anti-Nok (1:200; generated in-house, Zou et al., 2008), anti-Pals1 (1:2000 for immunoblotting; Millipore 07-708), anti-Ponli (1:200; generated in-house, Zou et al., 2010), anti-Crb1 (1:200; generated in-house, Zou et al., 2012), anti-Crb2a (1:200; generated in-house in rabbit, Zou et al., 2012), anti-Crb2b (1:200; generated in-house, Zou et al., 2012), anti-Crb2a (1:200; mouse monoclonal antibody, ZIRC zs-4), anti-aPKC (1:200; Santa Cruz, sc216) and anti-Rab11 (1:100; CST2413s). The polyclonal antibodies recognize the residues surrounding Arg184 of human Rab11a protein. Alexa Fluor 488 Phalloidin (1:300, Life Tech A12379) and Alexa Fluor 647 Phalloidin (1:100; Life Tech A22287) were used to visualize F-actin. Dapi (Thermo Fisher Scientific, D3571) was used to stain nuclei. Immunohistochemistry was performed using the procedure described previously (Zou et al., 2008). Confocal microscopy was performed using a Nikon A1 confocal microscope. Adobe Photoshop 7.0 was used for subsequent image processing. For all immunohistochemistry experiments, we repeated each experiment at least three times, and at least 10 embryos were analyzed for each experiment.

Transmission electron microscopy

The embryos at desired developmental stage were fixed in 2% electron microscope (EM) grade glutaraldehyde plus 2% paraformaldehyde in 0.1 M PBS (pH 7.3) at 4°C, rinsed in PBS, postfixed with 1% OsO_4 and 0.1% $K_3Fe(CN)_6$, dehydrated through a graded series of ethanol and embedded in Epon (Energy Beam Sciences, East Granby, CT, USA). Ultrathin tissue sections (65 nm) were stained with 2% uranyl acetate and Reynold's lead citrate and then examined with a Hitachi Model H-7650 transmission electron microscope.

Cell culture, transfections and immunofluorescence

HEK293T and MDCK cells were obtained from ATCC and cultured in DMEM medium with 10% fetal bovine serum (FBS) at 37°C in 5% CO_2 (v/v). For the immunofluorescence experiments, HEK293T cells were transfected with the specified plasmids for 24 h (plasmids expressing eGFP; Crb2a and Nok; Crb2a, Nok and mCherry-Rab11a; Crb2a, Nok and mCherry-Rab11a S25N; or aPKCλ-eGFP and Pard6γb) using Xtremegene HP (Roche) or polyethylenimine (PEI; Polysciences) transfection reagents. The transfected cells were fixed in 4% paraformaldehyde, permeabilized, blocked in 2% BSA and 0.1% Triton X-100 in PBS for 30 min, and incubated sequentially with primary antibodies anti-Crb2a or anti-β-catenin and Alexa Flour-labeled secondary antibodies with extensive washing. Immunofluorescence images were obtained using the Nikon A1 confocal microscope.

Co-immunoprecipitation and immunoblotting

HEK293T cells transfected for 24 h with specific plasmids encoding N-terminal Myc-, HA- and FLAG-tagged Rab11a, $Crb2a^{\Delta EX}$, Nok, Par5ζ, Par5θ, aPKCλ, Pard6γb and Pard3 were lysed using modified Myc lysis buffer (MLB) (20 mM Tris-Cl, 200 mM NaCl, 10 mM NaF, 1 mM NaV_2O_4, 1% NP-40, 20 mM β-glycerophosphate and protease inhibitor, pH 7.5). Cell lysates were then subjected to immunoprecipitation using anti-FLAG or anti-HA antibodies for transfected proteins, or using anti-Rab11/PALS1 antibodies for the endogenous proteins of MDCK cells. After two or three washes with MLB, adsorbed proteins in beads were resolved with 1× SDS loading buffer and analyzed by SDS-PAGE and immunoblotting with indicated antibodies. Cell lysates were also analyzed by SDS-PAGE and immunoblotting to control protein abundance.

Quantifications

Adobe Photoshop 7.0 (Adobe) was used to quantify the length of adhesion plaques imaged by TEM and to quantify the fluorescence intensity imaged by confocal microscopy. Prism 6.0b (Graphpad) was used to plot graphs and for statistical analyses. The value for adhesion plaques per epithelium shown in Fig. 2F and Fig. 5K was defined by the sum of the number of adhesion plaques divided by the number of epithelial cells for each lens. We compared the membrane-associated β-catenin intensity in the transfection-positive cells (Fig. 4F-J, marked by *) with that in the transfection-negative neighbor cells (Fig. 4F-J, marked by #). The relative intensity of membrane-associated β-catenin shown in Fig. 4K was defined by the intensity in the cells in Fig. 4F-J marked with * divided by that in the cells marked by #. The co-expressed eGFP-Rab11a and Nok-mCherry proteins were spread broadly in MDCK cells, with aggregation in Golgi. The images were read with Adobe Photoshop 7.0 and the percentage of triple positive foci shown in Fig. 4N was defined by the number of Rab11/Nok/GM130 triple positive foci divided by the total number of Rab11-positive foci or Nok-positive foci. The value of apical/basal relative intensity shown in Fig. 5H and Fig. 6I,K was defined by the fluorescence intensity of the apical spot at the vertex point between two epithelial cells (green spot, Fig. 5G) divided by the fluorescence intensity of the basal spot (red spot, same size as the green spot). In each lens, five anterior epithelial cells and eight lateral epithelial cells (four dorsal and four ventral cells) were measured. A total of 20 lenses from 10 embryos were imaged and used for the quantification analyses. The ratio of fiber cells to epithelial cells shown in Fig. S4H was defined by the nuclei number of inner lens cells divided by the nuclei number of epithelial cells in the same lens.

Statistics

In this study, five embryos for TEM-related quantitative analyses and at least 10 embryos for immunohistochemistry-related quantitative analyses were used for each experiment. Immunohistochemistry, time-lapse imaging and cell culture experiments were repeated a minimum of three independent times to ensure reproducibility. Data are expressed as mean±s.e.m. Differences were analyzed by two-tailed Student's *t*-test using Prism 6 (GraphPad Software, La Jolla, CA); P values <0.05 were considered significant. No statistical method was used to predetermine sample size. The investigators were not blinded to allocation during experiments and outcome assessment.

Acknowledgements

We are grateful to J. Peng and X. Feng (Zhejiang University) for valuable suggestions.

Competing interests

The authors declare no competing or financial interests.

Author contributions

Conceptualization: X.T., J.Z.; Methodology: J.Z.; Validation: J.Z.; Formal analysis: J.Z.; Investigation: Y.H., Y.Z., Y.Y., M.Z., K.W., Z.K., J.L., Q.Z., J.Z.; Resources: B.A.L., J.Z.; Data curation: J.Z.; Writing - original draft: J.Z.; Writing - review & editing:

Y.H., Y.Z., Y.Y., M.Z., K.W., Q.Z., X.T., P.X., B.A.L., K.Y., J.Z.; Supervision: P.X., K.Y., J.Z.; Project administration: J.Z.; Funding acquisition: X.T., K.Y., J.Z.

Funding

This work was supported by the Natural Science Foundation of Zhejiang Province (LZ15H120001 to J.Z.), the National Natural Science Foundation of China (81770938 to J.Z., 81800807 to X.T. and 81570822 to K.Y.) and the Fundamental Research Funds for the Central Universities (2016FZA7010 and 2017FZA7001 to J.Z., and 2017FZA7002 to X.T.).

Supplementary information

Supplementary information available online at
https://dev.biologists.org/lookup/doi/10.1242/dev.184457.supplemental

Peer review history

The peer review history is available online at
https://dev.biologists.org/lookup/doi/10.1242/dev.184457.reviewer-comments.pdf

References

Aguilar-Aragon, M., Elbediwy, A., Foglizzo, V., Fletcher, G. C., Li, V. S. W. and Thompson, B. J. (2018). Pak1 kinase maintains apical membrane identity in epithelia. *Cell Rep.* **7**, 1639-1646. doi:10.1016/j.celrep.2018.01.060

Apodaca, G., Gallo, L. I. and Bryant, D. M. (2012). Role of membrane traffic in the generation of epithelial cell asymmetry. *Nat. Cell Biol.* **14**, 1235-1243. doi:10.1038/ncb2635

Arora, P., Dongre, S., Raman, R. and Sonawane, M. (2020). Stepwise polarisation of developing bilayered epidermis is mediated by aPKC and E-cadherin in zebrafish. *eLife* **9**, e49064. doi:10.7554/eLife.49064

Balda, M. S. and Matter, K. (2016). Tight junctions as regulators of tissue remodelling. *Curr. Opin. Cell Biol.* **42**, 94-101. doi:10.1016/j.ceb.2016.05.006

Barbieri, M. A., Roberts, R. L., Mukhopadhyay, A. and Stahl, P. D. (1996). Rab5 regulates the dynamics of early endosome fusion. *Biocell* **20**, 331-338.

Betschinger, J., Mechtler, K. and Knoblich, J. A. (2003). The Par complex directs asymmetric cell division by phosphorylating the cytoskeletal protein Lgl. *Nature* **422**, 326-330. doi:10.1038/nature01486

Bruser, L. and Bogdan, S. (2017). Adherens junctions on the move-membrane trafficking of e-cadherin. *Cold Spring Harb. Perspect. Biol.* **9**, a029140. doi:10.1101/cshperspect.a029140

Bryant, D. M., Datta, A., Rodríguez-Fraticelli, A. E., Peränen, J., Martin-Belmonte, F. and Mostov, K. E. (2010). A molecular network for de novo generation of the apical surface and lumen. *Nat. Cell Biol.* **12**, 1035-1045. doi:10.1038/ncb2106

Bulgakova, N. A. and Knust, E. (2009). The Crumbs complex: from epithelial-cell polarity to retinal degeneration. *J. Cell Sci.* **122**, 2587-2596. doi:10.1242/jcs.023648

Campanale, J. P., Sun, T. Y. and Montell, D. J. (2017). Development and dynamics of cell polarity at a glance. *J. Cell Sci.* **130**, 1201-1207. doi:10.1242/jcs.188599

Chavrier, P., Parton, R. G., Hauri, H. P., Simons, K. and Zerial, M. (1990). Localization of low molecular weight GTP binding proteins to exocytic and endocytic compartments. *Cell* **62**, 317-329. doi:10.1016/0092-8674(90)90369-P

Chen, J. and Zhang, M. (2013). The Par3/Par6/aPKC complex and epithelial cell polarity. *Exp. Cell Res.* **319**, 1357-1364. doi:10.1016/j.yexcr.2013.03.021

Chen, W., Feng, Y., Chen, D. and Wandinger-Ness, A. (1998). Rab11 is required for trans-golgi network-to-plasma membrane transport and a preferential target for GDP dissociation inhibitor. *Mol. Biol. Cell* **9**, 3241-3257. doi:10.1091/mbc.9.11.3241

Clark, B. S., Winter, M., Cohen, A. R. and Link, B. A. (2011). Generation of Rab-based transgenic lines for in vivo studies of endosome biology in zebrafish. *Dev. Dyn.* **240**, 2452-2465. doi:10.1002/dvdy.22758

Fletcher, G. C., Lucas, E. P., Brain, R., Tournier, A. and Thompson, B. J. (2012). Positive feedback and mutual antagonism combine to polarize Crumbs in the Drosophila follicle cell epithelium. *Curr. Biol.* **22**, 1116-1122. doi:10.1016/j.cub.2012.04.020

Flores-Benitez, D. and Knust, E. (2015). Crumbs is an essential regulator of cytoskeletal dynamics and cell-cell adhesion during dorsal closure in Drosophila. *eLife* **4**, e07398. doi:10.7554/eLife.07398

Gorvel, J.-P., Chavrier, P., Zerial, M. and Gruenberg, J. (1991). rab5 controls early endosome fusion in vitro. *Cell* **64**, 915-925. doi:10.1016/0092-8674(91)90316-Q

Greiling, T. M. S. and Clark, J. I. (2009). Early lens development in the zebrafish: a three-dimensional time-lapse analysis. *Dev. Dyn.* **238**, 2254-2265. doi:10.1002/dvdy.21997

Halaoui, R. and McCaffrey, L. (2015). Rewiring cell polarity signaling in cancer. *Oncogene* **34**, 939-950. doi:10.1038/onc.2014.59

Harris, T. J. C. and Peifer, M. (2007). aPKC controls microtubule organization to balance adherens junction symmetry and planar polarity during development. *Dev. Cell* **12**, 727-738. doi:10.1016/j.devcel.2007.02.011

Harris, K. P. and Tepass, U. (2008). Cdc42 and Par proteins stabilize dynamic adherens junctions in the Drosophila neuroectoderm through regulation of apical endocytosis. *J. Cell Biol.* **183**, 1129-1143. doi:10.1083/jcb.200807020

Harris, T. J. C. and Tepass, U. (2010). Adherens junctions: from molecules to morphogenesis. *Nat. Rev. Mol. Cell Biol.* **11**, 502-514. doi:10.1038/nrm2927

Horgan, C. P. and McCaffrey, M. W. (2011). Rab GTPases and microtubule motors. *Biochem. Soc. Trans.* **39**, 1202-1206. doi:10.1042/BST0391202

Horne-Badovinac, S., Lin, D., Waldron, S., Schwarz, M., Mbamalu, G., Pawson, T., Jan, Y.-N., Stainier, D. Y. R. and Abdelilah-Seyfried, S. (2001). Positional cloning of heart and soul reveals multiple roles for PKCλ in zebrafish organogenesis. *Curr. Biol.* **11**, 1492-1502. doi:10.1016/S0960-9822(01)00458-4

Hosono, C., Matsuda, R., Adryan, B. and Samakovlis, C. (2015). Transient junction anisotropies orient annular cell polarization in the Drosophila airway tubes. *Nat. Cell Biol.* **17**, 1569-1576. doi:10.1038/ncb3267

Hsu, Y.-C., Willoughby, J. J., Christensen, A. K. and Jensen, A. M. (2006). Mosaic Eyes is a novel component of the Crumbs complex and negatively regulates photoreceptor apical size. *Development* **133**, 4849-4859. doi:10.1242/dev.02685

Hurd, T. W., Gao, L., Roh, M. H., Macara, I. G. and Margolis, B. (2003). Direct interaction of two polarity complexes implicated in epithelial tight junction assembly. *Nat. Cell Biol.* **5**, 137-142. doi:10.1038/ncb923

Imai, F., Yoshizawa, A., Fujimori-Tonou, N., Kawakami, K. and Masai, I. (2010). The ubiquitin proteasome system is required for cell proliferation of the lens epithelium and for differentiation of lens fiber cells in zebrafish. *Development* **137**, 3257-3268. doi:10.1242/dev.053124

Joberty, G., Petersen, C., Gao, L. and Macara, I. G. (2000). The cell-polarity protein Par6 links Par3 and atypical protein kinase C to Cdc42. *Nat. Cell Biol.* **2**, 531-539. doi:10.1038/35019573

Klebes, A. and Knust, E. (2000). A conserved motif in Crumbs is required for E-cadherin localisation and zonula adherens formation in Drosophila. *Curr. Biol.* **10**, 76-85. doi:10.1016/S0960-9822(99)00277-8

Lanzetti, L. (2007). Actin in membrane trafficking. *Curr. Opin. Cell Biol.* **19**, 453-458. doi:10.1016/j.ceb.2007.04.017

Laprise, P., Beronja, S., Silva-Gagliardi, N. F., Pellikka, M., Jensen, A. M., McGlade, C. J. and Tepass, U. (2006). The FERM protein Yurt is a negative regulatory component of the Crumbs complex that controls epithelial polarity and apical membrane size. *Dev. Cell* **11**, 363-374. doi:10.1016/j.devcel.2006.06.001

Morais-de-Sá, E., Mirouse, V. and St Johnston, D. (2010). aPKC phosphorylation of Bazooka defines the apical/lateral border in Drosophila epithelial cells. *Cell* **141**, 509-523. doi:10.1016/j.cell.2010.02.040

Nieto, M. A., Huang, R. Y.-J., Jackson, R. A. and Thiery, J. P. (2016). Emt: 2016. *Cell* **166**, 21-45. doi:10.1016/j.cell.2016.06.028

Omori, Y. and Malicki, J. (2006). oko meduzy and related crumbs genes are determinants of apical cell features in the vertebrate embryo. *Curr. Biol.* **16**, 945-957. doi:10.1016/j.cub.2006.03.058

Park, B., Alves, C. H., Lundvig, D. M., Tanimoto, N., Beck, S. C., Huber, G., Richard, F., Klooster, J., Andlauer, T. F. M., Swindell, E. C. et al. (2011). PALS1 is essential for retinal pigment epithelium structure and neural retina stratification. *J. Neurosci.* **31**, 17230-17241. doi:10.1523/JNEUROSCI.4430-11.2011

Penkert, R. R., DiVittorio, H. M. and Prehoda, K. E. (2004). Internal recognition through PDZ domain plasticity in the Par-6-Pals1 complex. *Nat. Struct. Mol. Biol.* **11**, 1122-1127. doi:10.1038/nsmb839

Ramkumar, N., Omelchenko, T., Silva-Gagliardi, N. F., McGlade, C. J., Wijnholds, J. and Anderson, K. V. (2016). Crumbs2 promotes cell ingression during the epithelial-to-mesenchymal transition at gastrulation. *Nat. Cell Biol.* **18**, 1281-1291. doi:10.1038/ncb3442

Roeth, J. F., Sawyer, J. K., Wilner, D. A. and Peifer, M. (2009). Rab11 helps maintain apical crumbs and adherens junctions in the Drosophila embryonic ectoderm. *PLoS ONE* **4**, e7634. doi:10.1371/journal.pone.0007634

Scott, C. C., Vacca, F. and Gruenberg, J. (2014). Endosome maturation, transport and functions. *Semin. Cell Dev. Biol.* **31**, 2-10. doi:10.1016/j.semcdb.2014.03.034

Simmons, N. L. (1982). Cultured monolayers of MDCK cells: a novel model system for the study of epithelial development and function. *Gen. Pharmacol.* **13**, 287-291. doi:10.1016/0306-3623(82)90047-7

Sobajima, T., Yoshimura, S.-I., Iwano, T., Kunii, M., Watanabe, M., Atik, N., Mushiake, S., Morii, E., Koyama, Y., Miyoshi, E. et al. (2014). Rab11a is required for apical protein localisation in the intestine. *Biol. Open* **4**, 86-94. doi:10.1242/bio.20148532

Sotillos, S., Díaz-Meco, M. T., Caminero, E., Moscat, J. and Campuzano, S. (2004). DaPKC-dependent phosphorylation of Crumbs is required for epithelial cell polarity in Drosophila. *J. Cell Biol.* **166**, 549-557. doi:10.1083/jcb.200311031

Stenmark, H. (2009). Rab GTPases as coordinators of vesicle traffic. *Nat. Rev. Mol. Cell Biol.* **10**, 513-525. doi:10.1038/nrm2728

Stenmark, H., Parton, R. G., Steele-Mortimer, O., Lütcke, A., Gruenberg, J. and Zerial, M. (1994). Inhibition of rab5 GTPase activity stimulates membrane fusion in endocytosis. *EMBO J.* **13**, 1287-1296. doi:10.1002/j.1460-2075.1994.tb06381.x

Tepass, U. (1996). Crumbs, a component of the apical membrane, is required for zonula adherens formation in primary epithelia of Drosophila. *Dev. Biol.* **177**, 217-225. doi:10.1006/dbio.1996.0157

Tepass, U. (2012). The apical polarity protein network in Drosophila epithelial cells: regulation of polarity, junctions, morphogenesis, cell growth, and survival. *Annu. Rev. Cell Dev. Biol.* **28**, 655-685. doi:10.1146/annurev-cellbio-092910-154033

Thisse, B., Heyer, V., Lux, A., Alunni, A., Degrave, A., Seiliez, I., Kirchner, J., Parkhill, J.-P. and Thisse, C. (2004). Spatial and temporal expression of the zebrafish genome by large-scale in situ hybridization screening. *Meth. Cell. Biol.* **77**, 505-519. doi:10.1016/s0091-679x(04)77027-2

Überall, F., Hellbert, K., Kampfer, S., Maly, K., Villunger, A., Spitaler, M., Mwanjewe, J., Baier-Bitterlich, G., Baier, G. and Grunicke, H. H. (1999). Evidence that atypical protein kinase C-lambda and atypical protein kinase C-zeta participate in Ras-mediated reorganization of the F-actin cytoskeleton. *J. Cell Biol.* **144**, 413-425. doi:10.1083/jcb.144.3.413

Ullrich, O., Reinsch, S., Urbé, S., Zerial, M. and Parton, R. G. (1996). Rab11 regulates recycling through the pericentriolar recycling endosome. *J. Cell Biol.* **135**, 913-924. doi:10.1083/jcb.135.4.913

van de Pavert, S. A., Meuleman, J., Malysheva, A., Aartsen, W. M., Versteeg, I., Tonagel, F., Kamphuis, W., McCabe, C. J., Seeliger, M. W. and Wijnholds, J. (2007). A single amino acid substitution (Cys249Trp) in Crb1 causes retinal degeneration and deregulates expression of pituitary tumor transforming gene Pttg1. *J. Neurosci.* **27**, 564-573. doi:10.1523/JNEUROSCI.3496-06.2007

Wei, Z., Li, Y., Ye, F. and Zhang, M. (2015). Structural basis for the phosphorylation-regulated interaction between the cytoplasmic tail of cell polarity protein crumbs and the actin-binding protein moesin. *J. Biol. Chem.* **290**, 11384-11392. doi:10.1074/jbc.M115.643791

Winter, J. F., Höpfner, S., Korn, K., Farnung, B. O., Bradshaw, C. R., Marsico, G., Volkmer, M., Habermann, B. and Zerial, M. (2012). Caenorhabditis elegans screen reveals role of PAR-5 in RAB-11-recycling endosome positioning and apicobasal cell polarity. *Nat. Cell Biol.* **14**, 666-676. doi:10.1038/ncb2508

Woichansky, I., Beretta, C. A., Berns, N. and Riechmann, V. (2016). Three mechanisms control E-cadherin localization to the zonula adherens. *Nat. Commun.* **7**, 10834. doi:10.1038/ncomms10834

Yonemura, S. (2011). Cadherin-actin interactions at adherens junctions. *Curr. Opin. Cell Biol.* **23**, 515-522. doi:10.1016/j.ceb.2011.07.001

Zou, J., Lathrop, K. L., Sun, M. and Wei, X. (2008). Intact retinal pigment epithelium maintained by Nok is essential for retinal epithelial polarity and cellular patterning in zebrafish. *J. Neurosci.* **28**, 13684-13695. doi:10.1523/JNEUROSCI.4333-08.2008

Zou, J., Yang, X. and Wei, X. (2010). Restricted localization of ponli, a novel zebrafish MAGUK-family protein, to the inner segment interface areas between green, red, and blue cones. *Invest. Ophthalmol. Vis. Sci.* **51**, 1738-1746. doi:10.1167/iovs.09-4520

Zou, J., Wang, X. and Wei, X. (2012). Crb apical polarity proteins maintain zebrafish retinal cone mosaics via intercellular binding of their extracellular domains. *Dev. Cell* **22**, 1261-1274. doi:10.1016/j.devcel.2012.03.007

Zou, J., Wen, Y., Yang, X. and Wei, X. (2013). Spatial-temporal expressions of Crumbs and Nagie oko and their interdependence in zebrafish central nervous system during early development. *Int. J. Dev. Neurosci.* **31**, 770-782. doi:10.1016/j.ijdevneu.2013.09.005